SOIL MOISTURE CONTENT ESTIMATION FROM HYPERSPECTRAL REMOTE SENSING DATA

Ketaki Vinay Jambhali, Bikram Koirala, Zakaria Bnoulkacem, Paul Scheunders

Imec-Visionlab, Department of Physics, University of Antwerp (CDE), Universiteitsplein 1, B-2610 Antwerp

ABSTRACT

Because of its significant absorption power, particularly in the SWIR optical region (e.g., absorption features around 1400 and 1900 nm), water dominates the optical reflectance properties of water-bearing materials. This allows us to study a material's water-related features, such as its moisture content from optical reflectance. In this study, we proposed a framework to estimate soil moisture content from hyperspectral remote sensing data. Validation is performed on Hyperion hyperspectral satellite imagery and ground-truth data from the Soil Moisture Network database.

***Index Terms*—** Hyperspectral, Hyperion EO-1, soil moisture content, machine learning, remote sensing

1. INTRODUCTION

In studies of the regional water cycle, agricultural irrigation management, climate change, and environmental monitoring, soil moisture is an essential variable [1]. The term "soil moisture" refers to the water existing on land surfaces that is present in the pores of the soil. Multiple factors, including the type of soil and nearby vegetation, as well as meteorological conditions, affect the amount of soil moisture [2]. In turn, a variety of soil and plant dynamics are impacted by soil moisture levels [3]. Traditional methods, such as the thermo-gravimetric technique and the calcium-carbide approach require both field sampling and laboratory analysis [4]. Although these approaches have high accuracy, they also have drawbacks, including complicated sampling procedures and the need for a large number of repeated experiments [5]. Moreover, most of these techniques do not allow for monitoring of the spatial distribution of soil moisture on a wide scale.

In comparison to these traditional methods, remote sensing technology allows for monitoring large-scale near-surface soil moisture. Currently, optical, thermal, and microwave remote-sensing sensors are used to measure soil moisture content.

Microwave remote sensing allows for a continuous, large-scale soil moisture estimation. Wide-scale soil moisture data have been collected by the Soil Moisture Active Passive (SMAP) and Soil Moisture and Ocean Salinity (SMOS) satellite missions [6], from which global-scale soil moisture can be measured [7]. Although numerous algorithms have been developed to estimate soil moisture content from microwave radiation, the resulting data products often exhibit limited spatial resolution (10–20 km [8]), even when collected from airborne systems ([9]), making them less suitable for monitoring e.g., small catchment areas ([10]).

With thermal infrared remote sensing, wavelengths ranging from approximately 3500 nm to 14,000 nm are used to estimate the soil moisture content. The use of thermal remote sensing for estimating soil moisture has been restricted in the past due to high acquisition costs. Currently, high-spatial and temporal-resolution thermal images are affordable thanks to advancements in low-cost remote-sensing platforms such as unmanned aerial systems (UAVs), which have contributed to understanding the variability of soil conditions [11]. Often, the methods that exploit thermal infrared remote sensing images are empirical in nature and depend upon local meteorological factors, such as wind speed, air temperature, and humidity [12].

Due to the high absorption power of water, soil moisture has a significant impact on the reflection of soil surfaces in the near-infrared (NIR) (700-1100 nm) and shortwave infrared (SWIR) (1100-2500 nm) wavelength ranges. To exploit this property of water, the reflectance in the 350–2500 nm range has been utilized in optical remote sensing to estimate soil moisture [12]. In contrast to active microwave sensors, the primary benefit of using the optical part of electromagnetic radiation is that solar radiation acts as a natural illumination source [12]. In [13], it was experimentally demonstrated that spectral reflectance acquired in the SWIR wavelength regions is more suitable to accurately predict the soil moisture content. In [12], the Sadeghi model (SM) was derived from the Kubelka–Munk theory. This model estimates the soil moisture of moist soil by making use of the spectral reflectance of dry and saturated soil. The major drawback of models such as SM is that they are not invariant to the illumination and viewing angles. To tackle this challenge, in recent work [14], we have proposed a methodology (NRAL) that is invariant to the changes in the acquisition and illumination conditions.

NRAL has been validated extensively on laboratory data. In this work, we wanted to explore its use in remote sensing applications, by estimating soil moisture content from Hyperion hyperspectral images.

2. DATASETS

2.1. Hyperspectral dataset

In this work, we analyzed hyperspectral images acquired by the Hyperion sensor attached to the Earth Observing-1 (EO-1) spacecraft. Hyperion acquires spectral reflectances of the Earth's surface in 242 unique spectral channels ranging from 357 to 2576 nm with a 10-nm bandwidth. The spatial resolution is approximately 30 m. We downloaded the hyperspectral images from the USGS Earth Explorer, referred to as the Level 1R data set. The following two steps have been performed to convert raw digital numbers (DN) acquired by the sensor to the surface reflectance: a) Radiometric calibration and b) Atmospheric correction. As atmospheric effects can distort the measured reflectance values, making it challenging to accurately interpret the surface properties, atmospheric correction is crucial for obtaining accurate surface reflectance measurements in remote sensing imagery [15]. In this work, we applied QUick Atmospheric Correction (QUAC) [16] to convert radiance into surface reflectance.

2.2. Soil moisture dataset

In order to validate estimated soil moisture content, ground-measured soil moisture content is required. In this work, we utilized the International Soil Moisture Network (ISMN) database. ISMN is an international cooperation to establish and maintain a global in-situ soil moisture database. ISMN gathers in-situ soil moisture data sets, shared voluntarily by different data organizations, and makes them accessible through a centralized web interface. ISMN comprises multiple networks (77 networks as of August 2023), each consisting of several stations. These networks range from networks with a single station to networks with more than 400 stations, encompassing a variety of terrain types as well as periods, and have variable levels of data update frequency. All measurements of soil moisture submitted to the ISMN are converted to volumetric soil moisture (m^3/m^3) [17].

2.3. Final dataset

Although extensive ground-measured soil moisture datasets from ISMN are available, it remained challenging to obtain the required hyperspectral remote-sensing imagery covering the same spatial locations. Hyperion images were queried that matched the date and geographical coordinates of the ground truth stations from the ISMN networks. After filtering, we identified 21 ground truth stations that met our requirements (see Figure 1).

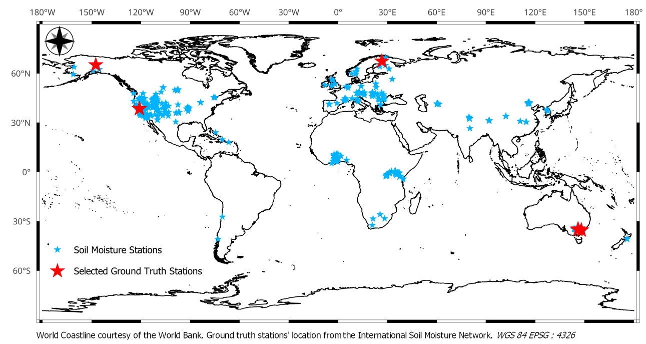

Fig. 1. Soil moisture ground truth stations. Blue stars denote all stations, while red stars indicate the 21 stations that align with Hyperion hyperspectral images, concentrated at 4 different locations.

As the spatial resolution of the hyperspectral dataset is 30 meters, each pixel covers a significant area on the ground. In this work, we assumed that each pixel corresponds to a specific station, whereas in reality, it encompasses a larger geographic extent. To minimize the uncertainty in the ground truth moisture data, spectra for each station were produced by averaging over a Region of Interest (ROI) of 3 $\times$ 3 pixels surrounding the soil moisture station. For each station, between 4-11 time instances could be used. In total, 115 spectra were obtained. For these spectra, the soil moisture content varies between 0-88 %. Figure 2 illustrates the proposed methodology.

3. RELEVANT METHODS

3.1. Sadeghi Model

The Sadeghi model (SM) [12], which is based on the Kubelka-Munk two-flux theory, is a radiative transfer model that is designed to relate the spectral reflectance of moist soil with its water content. This model establishes a connection between the reflectance of the moist soil, denoted as R with r, the ratio between the light absorption coefficient (m^{-1}) and the light scattering coefficient (m^{-1}) by the following equation:

$$R = 1 + r - \sqrt{r^2 + 2r} \tag{1}$$

Inverting the above equation yields:

$$r = \frac{(1-R)^2}{2R} \tag{2}$$

The soil moisture content is calculated in [12] as:

$$\theta = \frac{r - r_d}{r_s - r_d} \times \theta_s \tag{3}$$

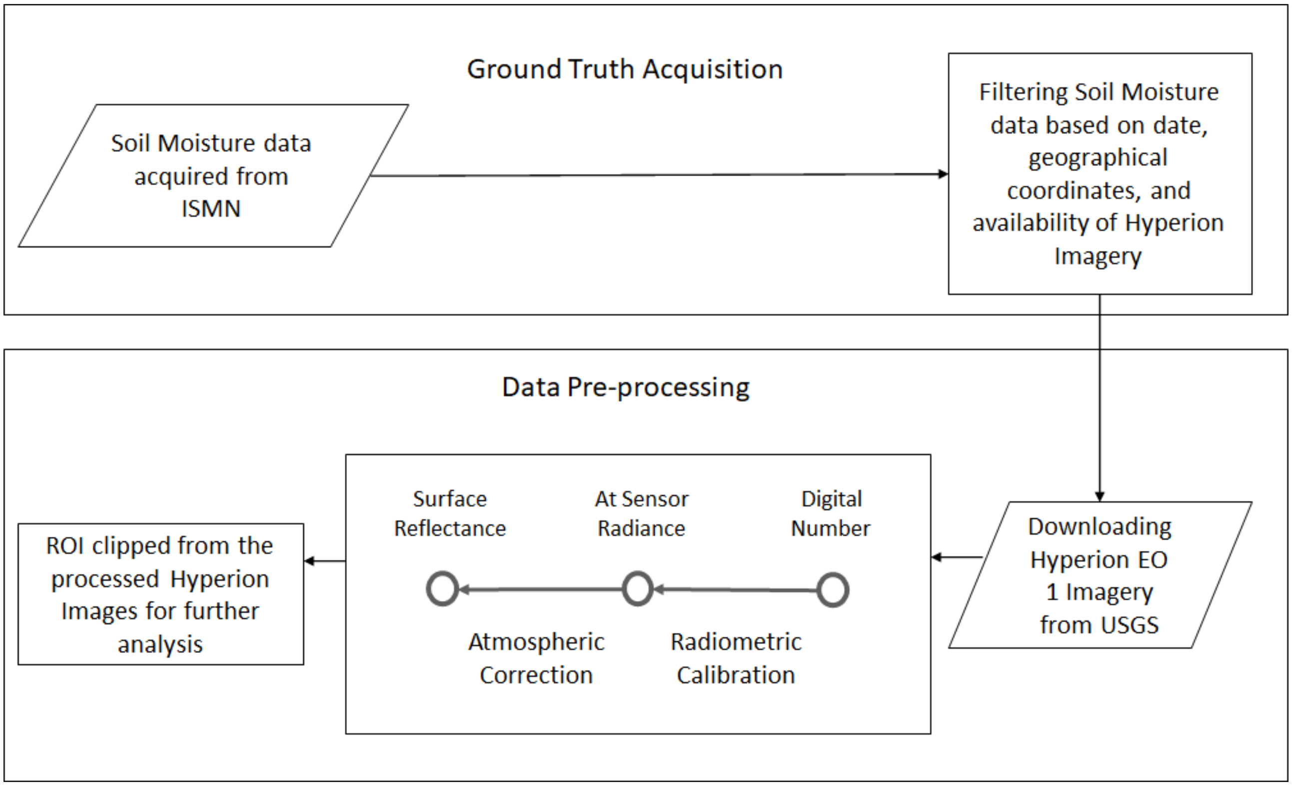

Fig. 2. Flowchart of the proposed method.

where θ and θ_s are the soil moisture contents of the moist and saturated soils, respectively, and r, r_d, and r_s are the absorption/scattering ratios of the moist, dry, and saturated soils, respectively. SM is applied on a single (in principle any) wavelength. A wavelength of 2210 nm was suggested in [12].

3.2. Normalized Relative Arc Lengths (NRAL)

In [14], a robust supervised method was proposed to accurately estimate the soil moisture content from spectral reflectance. The method assumes that moist soil is a binary mixture of air-dried and saturated soil samples. The method further assumes that the data manifold produced by a number of moist soil samples is a curve in spectral space between dry (R_d) and saturated (R_s) soils (endmembers). Estimating the moisture content of the moist soil sample then boils down to determining the relative arc length between moist soil and the two endmembers. To tackle spectral variability, the proposed method projects each input spectra onto the unit sphere. The arc length between any two spectra on the unit sphere is simply given by the angle between them and is given by the arc cosine of their dot product. However, it is not assured that all data points will lie on the arc connecting the two endmembers after projection. To determine the true arc lengths, the law of cosines was utilized. After some calculations, one obtains:

$$\cos b_1 = \frac{\sin(b_1+b_2)}{\sqrt{\left(\frac{\cos c'}{\cos c} - \cos(b_1+b_2)\right)^2 + \sin^2(b_1+b_2)}} \quad (4)$$

where c and c' denote the arc lengths between the moist soil and the endmembers, while b_1 and b_2 denote the true arc lengths between the moist soil and the endmembers, and $b_1 + b_2 = \arccos(\mathrm{R}_d^T \mathrm{R}_s)$. The relative arc lengths were then computed by:

$$\hat{a} = \begin{bmatrix} \frac{b_2}{b_1+b_2} \\ \frac{b_1}{b_1+b_2} \end{bmatrix} \quad (5)$$

In the final step, the soil moisture content was estimated by multiplying the relative arc length of the moist soil ($\hat{\mathbf{a}}$) by the soil moisture content of the saturated soil (θ_s) ($\hat{\theta} \rightarrow \hat{\mathbf{a}} \times \boldsymbol{\theta}_\mathbf{s}$).

4. EXPERIMENTS AND RESULTS

In this work, NRAL is validated for its application in soil moisture content estimation from remote sensing hyperspectral imagery. In the experiments, we compare its performance with the Sadhegi model (SM). Both methods require the spectra of an air-dried soil and saturated soil sample and their ground truth soil moisture content at each ground truth station. While the SM is designed to work at any of the SWIR wavelengths, we apply the reflectance value obtained at the wavelength 2210 nm, as recommended in [12]. For NRAL on the other hand, we utilized all spectral reflectance values between 1100 and 1700 nm.

All quantitative comparisons are provided by the root mean squared error (RMSE), i.e. the error between the estimated soil moisture content ($\hat{\theta}$) and the ground truth soil moisture content (θ):

$$\text{RMSE} = \sqrt{\frac{1}{n}\sum_{i=1}^{n}\left(\hat{\theta}_i - \theta_i\right)^2} \times 100 \qquad (6)$$

where n is the number of samples.

4.1. Experiment 1: Both dry and saturated samples are obtained from the same station

As both dry and saturated (wettest) samples from the same station are required, we checked all 21 stations and unfortunately found that the moisture content of the driest sample at most stations ranges from 4% to more than 41%. Only one station contained a dry sample and was suitable. On this station, only 6 spectra could be validated. In table 1, we show the obtained RMSE between the ground truth moisture content and the estimated ones on this one station. As can be observed, NRAL outperformed SM. The low error for both methods is partially due to the fact that the moisture content varies only between 0% and 2.89%.

Table 1. The results of different soil moisture estimation techniques in terms of RMSE (%).

	SM	NRAL
Experiment 1	1.44	**0.80**
Experiment 2	5.9×10^8	**32.24**

4.2. Experiment 2: Only a saturated sample is obtained from each station

In [14], Fig. 7, it was demonstrated that the relationship between the normalized relative arc length and the ground-measured soil moisture content is the same for different soils. This suggests that a data manifold generated by a number of moist soil samples is a unique curve that connects the dry and the saturated samples. Due to the high absorption power of water in the SWIR optical region, the spectral reflectance of the moist sample is dominated by water. This further suggests that dry samples obtained from different stations (if they would be available) are expected to be concentrated on one extreme of this curve. In contrast, the position of the saturated sample obtained from different stations can vary a lot on this curve due to variability in soil grain size (texture) and grain size distribution. To test this hypothesis and to expand the usable dataset, we relaxed the requirements and used the only dry sample in our dataset on all stations. The methods then only require a saturated sample from each station.

We then predicted the moisture content of all 115 samples. As expected, this relaxation deteriorates the performance of both methods (see table 1). However, while SM leads to entirely useless results, the results of NRAL still make sense.

In figure 3, a scatterplot shows the estimated moisture content versus ground-measured moisture content. Because of the unconstrained nature of the SM, the estimated moisture content varied between -650% and 5815425700 %. For visualization purposes, only estimations between 0% and 100% are shown. For the SM, only 64 samples fulfilled this criterion.

As can be observed, NRAL incorrectly estimated a soil moisture content of 0% for a number of data points (points on the y-axis). For these points, the method was not able to spectrally differentiate between a dry and a moist sample. A possible reason is that the ground truth soil moisture content was produced on bulk samples (approximately 5 cm thick samples), while the spectral reflectance only contains information from the top 100-200 μm thick layer of the soil. The correspondence between the reflectance data and the actual ground-truth soil moisture content is only correct when the sample exhibits a high degree of homogeneity. Probably for those samples, this is not the case.

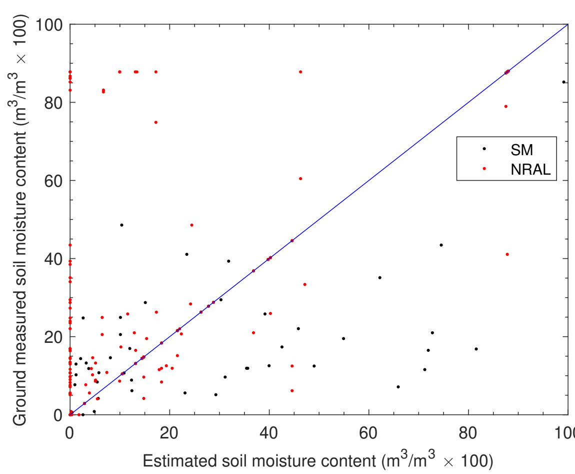

Fig. 3. Ground measured soil moisture content vs. estimated soil moisture content of moist soils

5. CONCLUSION

In this work, we studied the potential of NRAL to estimate the moisture content of soils from remote sensing hyperspectral data. For that, a framework was designed to align Hyperion hyperspectral images with ground truth soil moisture datasets. The experimental results indicate that the moisture content of moist soil can be accurately estimated from the remote sensing hyperspectral image when dry and saturated samples of the same spatial location are a priori available. When only saturated samples are available, the results are still meaningful compared to the Sadhegi model approach from the literature.

6. REFERENCES

[1] D. Datta, M. Paul, M. Murshed, S. Wei Teng, and L. Schmidtke, "Soil moisture, organic carbon, and nitrogen content prediction with hyperspectral data using regression models," *Sensors (Basel, Switzerland)*, vol. 22, 10 2022.

[2] Y. Wang, J. Yang, Y. Chen, G. Fang, W. Duan, Y. Li, and P. D. Maeyer, "Quantifying the effects of climate and vegetation on soil moisture in an arid area, china," *Water*, vol. 11, no. 4, 2019.

[3] S. Li and Y. Sawada, "Soil moisture-vegetation interaction from near-global in-situ soil moisture measurements," *Environmental Research Letters*, vol. 17, no. 11, pp. 114028, 2022.

[4] S. U. S. Lekshmi, D. N. Singh, and M. S. Baghini, "A critical review of soil moisture measurement," 2014.

[5] H. Wang, S. Gao, X. Yue, X. Cheng, Q. Liu, R. Min, H. Qu, and X. Hu, "Humidity-sensitive pmma fiber bragg grating sensor probe for soil temperature and moisture measurement based on its intrinsic water affinity," *Sensors*, vol. 21, 11 2021.

[6] D. Zhang and G. Zhou, "Estimation of soil moisture from optical and thermal remote sensing: A review," 8 2016.

[7] N. Ye et. al., "The soil moisture active passive experiments: Validation of the smap products in australia," *IEEE Transactions on Geoscience and Remote Sensing*, vol. 59, pp. 2922–2939, 4 2021.

[8] E. G. Njoku and D. Entekhabi, "Passive microwave remote sensing of soil moisture," *Journal of Hydrology*, vol. 184, no. 1, pp. 101–129, 1996, Soil Moisture Theories and Observations.

[9] J. Tian and W. D. Philpot, "Relationship between surface soil water content, evaporation rate, and water absorption band depths in swir reflectance spectra," *Remote Sensing of Environment*, vol. 169, pp. 280–289, 2015.

[10] D. Zhang and G. Zhou, "Estimation of soil moisture from optical and thermal remote sensing: A review," *Sensors (Basel, Switzerland)*, vol. 16, 2016.

[11] S. Khanal, J. Fulton, and S. Shearer, "An overview of current and potential applications of thermal remote sensing in precision agriculture," 6 2017.

[12] M. Sadeghi, S. B. Jones, and W. D. Philpot, "A linear physically-based model for remote sensing of soil moisture using short wave infrared bands," *Remote Sensing of Environment*, vol. 164, pp. 66–76, 7 2015.

[13] D. B. Lobell and G. P. Asner, "Moisture effects on soil reflectance," *Soil Science Society of America Journal*, vol. 66, pp. 722–727, 5 2002.

[14] B. Koirala, Z. Zahiri, and P. Scheunders, "A robust supervised method for estimating soil moisture content from spectral reflectance," *IEEE Transactions on Geoscience and Remote Sensing*, vol. 60, 2022.

[15] S. K. Khurshid and B. A. Abderrazak, "Preprocessing of eo-1 hyperion data remote sensing application in urban environment view project uavs/drones for vegetation and wetland mapping view project," 2006.

[16] L. S. Bernstein, X. Jin, B. Gregor, and S. M. A-Golden, "Quick atmospheric correction code: algorithm description and recent upgrades," *Optical Engineering*, vol. 51, pp. 111719, Nov. 2012.

[17] W. Dorigo et. al., "The international soil moisture network: Serving earth system science for over a decade," 11 2021.